

## Research



**Cite this article:** Muševič I. 2013 Nematic colloids, topology and photonics. *Phil Trans R Soc A* 371: 20120266.  
<http://dx.doi.org/10.1098/rsta.2012.0266>

One contribution of 14 to a Theo Murphy Meeting Issue 'New frontiers in anisotropic fluid–particle composites'.

### Subject Areas:

soft matter physics

### Keywords:

liquid crystals, photonics, topology

### Author for correspondence:

I. Muševič

e-mail: [igor.musevic@ijs.si](mailto:igor.musevic@ijs.si)

# Nematic colloids, topology and photonics

I. Muševič<sup>1,2</sup>

<sup>1</sup>J. Stefan Institute, Jamova 39, 1000 Ljubljana, Slovenia

<sup>2</sup>Faculty of Mathematics and Physics, University of Ljubljana, Jadranska 19, 1000 Ljubljana, Slovenia

We review and discuss recent progress in the field of nematic colloids, with an emphasis on possible future applications in photonics. The role of the topology is described, based on experimental manipulations of the topological defects in nematic colloids. The topology of the ordering field in nematics provides the forces between colloidal particles that are unique to these materials. We also discuss recent progress in the new field of active microphotonic devices based on liquid crystals (LCs), where chiral nematic microlasers and tuneable nematic microresonators are just two of the recently discovered examples. We conclude that the combination of topology and microphotonic devices based on LCs provides an interesting platform for future progress in the field of LCs.

## 1. Introduction

Civilization in the twenty-first century remains reliant on the great inventions of the nineteenth century. The famous names in natural sciences and engineering, such as Faraday, Maxwell, Edison, Tesla and many others, helped to create a world where electricity fuels our civilization. One of the foundations of our society is the exchange of information, which has evolved over the past 20 years to the level that is vital for our future development. The ever-increasing demands to share more information, not only at the local level but also on a worldwide scale, have produced a bottleneck in information exchange and processing. The existing infrastructure for managing the flow of information along photonic networks is based on protocols where electrically encoded information usually has to be translated into optical information, transmitted along optical fibres, and then converted back to electrically encoded information. This process is extremely costly in terms of energy as well as limiting

the speed of the signal propagation, which means new technologies for managing the flow of information in optical networks are required. The same problem has been experienced in the technology of microchip fabrication, where the gigahertz electrical signals cannot propagate without substantial delays and losses along the conductive transmission lines on the microchip, which then hinders data circulation inside the microchip itself.

It was proposed a long time ago that encoding, modifying and transmitting information with photons rather than electric charge could substantially enhance our capability for information exchange as well as the power of our computers. A good example is the transmission of information via photonic channels in optical waveguides, which have dramatically increased the capacity for information exchange. During the past 20 years or so, there has been a great deal of interest in developing new, photonic technologies for photonic-chip microfabrication. This interest is driven by the need to direct, multiplex, select and to re-direct photonically encoded information in future photonic microchip devices. Currently, the most promising technology seems to be the successful integration of photonics with standard CMOS microchip-fabrication techniques, where hybrid electric–photonic devices operating at several tens of gigahertz have been demonstrated. This approach, which uses step-by-step improvements to existing technology, mainly based on the photolithography and microfabrication of solid-state materials, will certainly solve some of the problems. However, the question is, can we invent and develop a new approach to photonic microdevices? One could imagine a platform that would enable the self-assembly of future photonic devices. It would be based on photon propagation in soft matter rather than solid matter, because soft matter is a fluid and therefore has the ability to self-assemble, while solid matter is frozen, immobile and unable to self-assemble easily. If this were not the case, we would be made of silicon instead of water.

Today, we are at an early stage of the realization of these ideas, and the aim of this article is to review some of the fundamental observations made over the past 8 years. It turns out that these are not just a collection of scattered phenomena, interesting in isolation, but indicate a firm coherence for the concept of soft-matter microphotonics.

## 2. The concept of a photonic crystal

The term ‘photonic crystal’ was proposed by Yablonovich & Gmitter in 1989 in their study [1]. A photonic crystal is one made of dielectric, transparent objects, where the unit cell is of the order of the wavelength of the light of interest (figure 1*a*). The optical properties of a photonic crystal are therefore analogous to the electronic properties of a solid crystal made up of atoms and can be explained on the basis of the general phenomena of wave propagation in periodic media. A solid crystal represents a periodic potential for the electrons, and so does the photonic crystal for photons. The spatial periodicity of the electronic potential is responsible for the band structure of the electronic levels. The same applies for light in a photonic crystal: because of the periodicity, the crystal must exhibit a ‘band structure’ for the allowed photonic states, shown in figure 1*b*. In other words, the dispersion relation for light propagating in a photonic crystal,  $\omega(\vec{k})$ , which links the frequency of the electromagnetic wave,  $\omega$ , to the wavevector of light,  $\vec{k}$ , should exhibit forbidden frequency gaps. This means that light with a frequency of oscillation in the forbidden gap cannot propagate inside the crystal, as there are no available states for such a process. As a result, light of a certain frequency falling on such a crystal is reflected from the crystal. This reflection may depend on the direction of propagation; if the light is reflected for all incident angles, then the band gap is a complete photonic band gap.

The concept of a photonic band gap in photonic crystals is a well-known phenomenon in liquid crystals (LCs). It can be observed in cholesteric (chiral nematic) LCs, which are made up of chiral organic molecules, spontaneously organized into a helically ordered phase. In this phase, the molecules are locally aligned parallel to each other along the director, but this direction is precessing, as we move perpendicular to the director. Optically, the phase is locally highly birefringent, with the optical axis pointing along the director. However, as the director

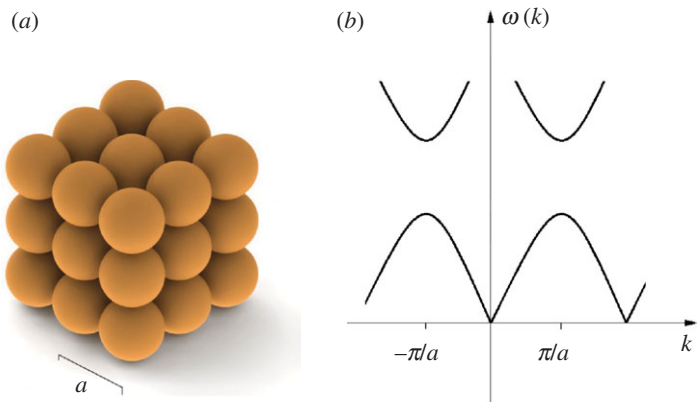


**Figure 1.** (a) A photonic crystal is a three-dimensional arrangement of dielectric objects with their mutual separation of the order of the wavelength of the light of interest. (b) The dispersion relation for light propagating in such a crystal is periodic in the reciprocal space. It exhibits forbidden gaps, where no light with frequency within the forbidden region can propagate. (Online version in colour.)

twists in space, so does the optical axis. This leads to an optically anisotropic material with a helicoidal precession of the optical axis in one direction, which gives rise to the one-dimensional photonic band gap of the cholesteric phase. A thin film of a cholesteric LC appears coloured when illuminated with white light. This is because it reflects light with the frequency inside the forbidden one-dimensional band gap and the cholesteric material appears coloured. Light waves of the same helicity as the handedness of the cholesteric twisted phase are reflected, while the light with the opposite helicity is transmitted.

Because of their band gap properties, photonic crystals are interesting not only for studying the fundamental phenomena of light emission and propagation, but also for photonic applications. A photonic crystal acts as a perfect mirror for monochromatic light with its frequency in the forbidden frequency gap. Such a perfect, lossless mirror could therefore be applied to control and guide photons along smartly designed photonic pathways. There has been immense interest since the invention of photonic crystals in the science and technology of the photonic crystal and there are various approaches to the question of how to produce such crystals. The fabrication of photonic crystals has been approached using a variety of techniques, such as directed colloidal crystallization on patterned surfaces [2], micromanipulation using a micromechanical laser [3] or optoelectronic tweezers [4], colloidal self-assembly via DNA hybridization [5] and microstructures produced by using conventional microelectronic photolithography [6].

### 3. Photonic crystals made of liquid crystals and colloids

It was demonstrated by Poulin *et al.* [7] that nematic LCs have the unusual ability to mediate forces between particles that are immersed in the nematic LC. Dispersions of solid particles in a nematic LC are called nematic colloids, while dispersions of fluid droplets or even gaseous bubbles in nematic LCs are called emulsions. The forces between the particles in the nematic LC are of elastic origin. When a particle with a well-defined surface anchoring of LC molecules is introduced into the LC, the molecules align along the curved and closed surface of the particle. This is a frustration for the LC molecules, as they have to align around the particle and at the same time they have to be homogeneously oriented far away from the particle. This inability to fill the space with a uniformly aligned nematic LC results in a strong elastic distortion of the nematic LC around the particle. This distortion is easily observed under a polarizing microscope and is presented in figure 2*a–e*. It is clear that there are two different symmetries of the surrounding

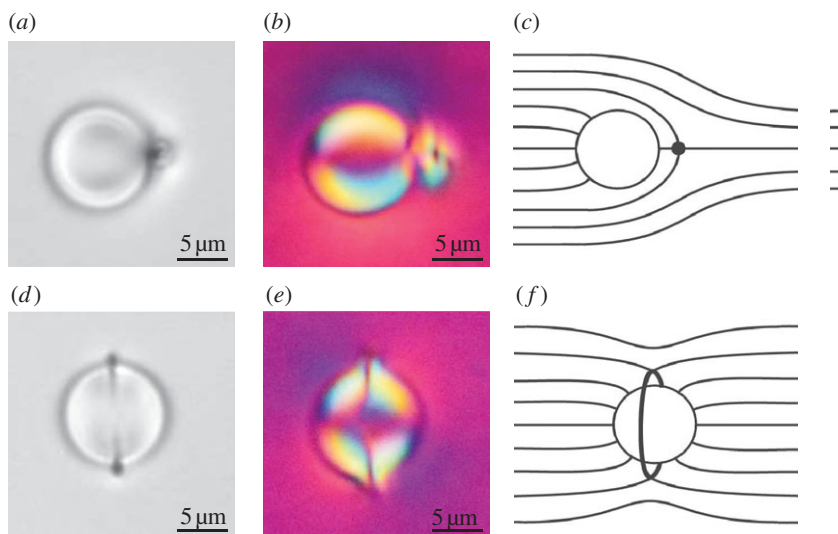


**Figure 2.** A silica microsphere, treated so as to align the LC molecules perpendicular to its surface, appears in the form of either a dipole (*a*) or a quadrupole (*d*). (*a,d*) Photographs taken without any polarizers. The small dot in (*a*) is the hedgehog topological defect. The ring, visible in (*d*), is the Saturn ring. It is a  $-1/2$  disclination ring, encircling the particle at the equator. The images in (*b*) and (*e*) are taken using crossed polarizers and the red ( $\lambda$ ) plate. (*c,d*) A schematic of the director-field distribution. (Online version in colour.)

nematic LC for normal surface-anchoring conditions. The first one has the symmetry of a dipole (figure 2*a–c*) and the second has the symmetry of a quadrupole (figure 2*d–f*), hence they are called dipolar and quadrupolar nematic colloids.

Because each colloidal particle is surrounded by an elastically distorted, nematic LC, the free energy of a pair of nematic colloids depends on their mutual separation. Changing the separation between the inserted particles changes the field of the elastic distortion in between and around them. Because the free energy depends on the separation, the force of elastic origin should act on each of the particles. This force is, in principle, of thermodynamic origin, as the changes in the elastic deformation are accompanied by changes in the degree and the nature of the order of the nematic LC. The force between nematic colloidal particles has been studied in detail by different groups [8–15], and it is sufficient to say that it is of long range (power-law dependence in a thick nematic) and very strong. For a particle diameter of  $1\ \mu\text{m}$ , the force depends on the separation and the angle of approach of another particle, but it is substantial over a separation of several micrometres, resulting in pair-interaction potential energies as high as several  $1000\ k_{\text{B}}T$  per micrometre particle. This is a huge energy compared with the van der Waals pair interaction in water-based colloids and is responsible for the extreme stability of the colloidal assemblies in a nematic LC.

The dipolar and quadrupolar forces between nematic colloidal particles were used to assemble one-dimensional colloidal chains (figure 3*a,b*) and two-dimensional nematic colloidal crystals of different symmetries [7,8,16,17], shown in figure 3. A two-dimensional colloidal crystal made up of dipolar colloids is presented in figure 3*c*. Such a crystal is assembled using the laser tweezer manipulation of individual particles [18]. These assemblies are very robust and can be transported as a whole. Several other two-dimensional colloidal crystals have been demonstrated, including quadrupolar colloidal crystals [16] and binary colloidal crystals made up of dipolar and quadrupolar colloids, shown in figure 3*f* [17]. When small and big colloidal particles are mixed together in the nematic LC, smaller particles tend to decorate the topological defects around bigger particles and hierarchical structures are formed, as presented in figure 3*e* [19]. In all these crystals and superstructures, topological point or loop defects play the role of a ‘binding glue’ for these structures. Without defects, the structures would not be stable and the defects determine the

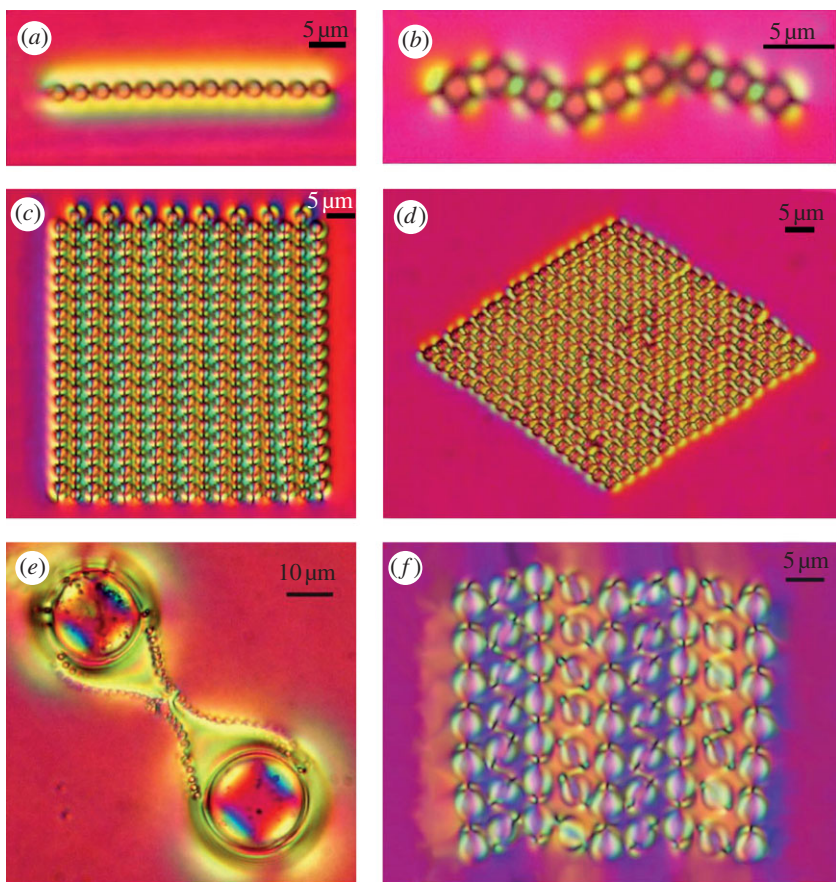


**Figure 3.** (a) One-dimensional chains of dipolar colloidal particles, and a kinked chain (b), made up of quadrupolar particles. Two-dimensional nematic colloidal crystals assembled from dipolar colloidal particles (c), quadrupolar colloidal particles (d) or a mixture of both (f). (e) Hierarchical colloidal structures are formed in a mixture of small and big colloidal particles, where smaller particles are trapped into the defect lines surrounding bigger particles. (Online version in colour.)

strength and symmetry of the binding-pair potential. However, when the nematic LC mediating the colloidal interaction is not homogeneous, but chiral (i.e. twisted), a new class of topology emerges that significantly changes the nature of the colloidal-pair potential. In a  $\pi/2$  twisted nematic cell, which is the most simple example of a chiral nematic LC, a pair of topological dipoles interacts in such a way that each topological point defect opens up into a small loop, and the two neighbouring loops merge into an escaped torus-type defect [8,20–22]. Such colloidal dimers then interact with each other and assemble into a square two-dimensional colloidal crystal.

The emergence of topological defects in nematic colloids is not only important for the interaction and binding of colloidal particles into stable and geometrically regular structures, as demonstrated in a number of studies; they are interesting objects by themselves [23–25]. The topological defects in nematic LCs are reminiscent of the phenomenon of the electric charge, because they seem to obey the law of conservation of the topological charge [26]. Although it is an appealing analogy, there are serious dilemmas in capturing the true nature of the topological charge attributed to these defects, as discussed recently by Čopar & Žumer [27]. Furthermore, it also seems that the topology, which was long considered as an abstract mathematical discipline with little connection to the physics of materials, suddenly becomes important for our understanding of the forces that are responsible for the self-organization of nematic colloids. This will be illustrated in more detail below.

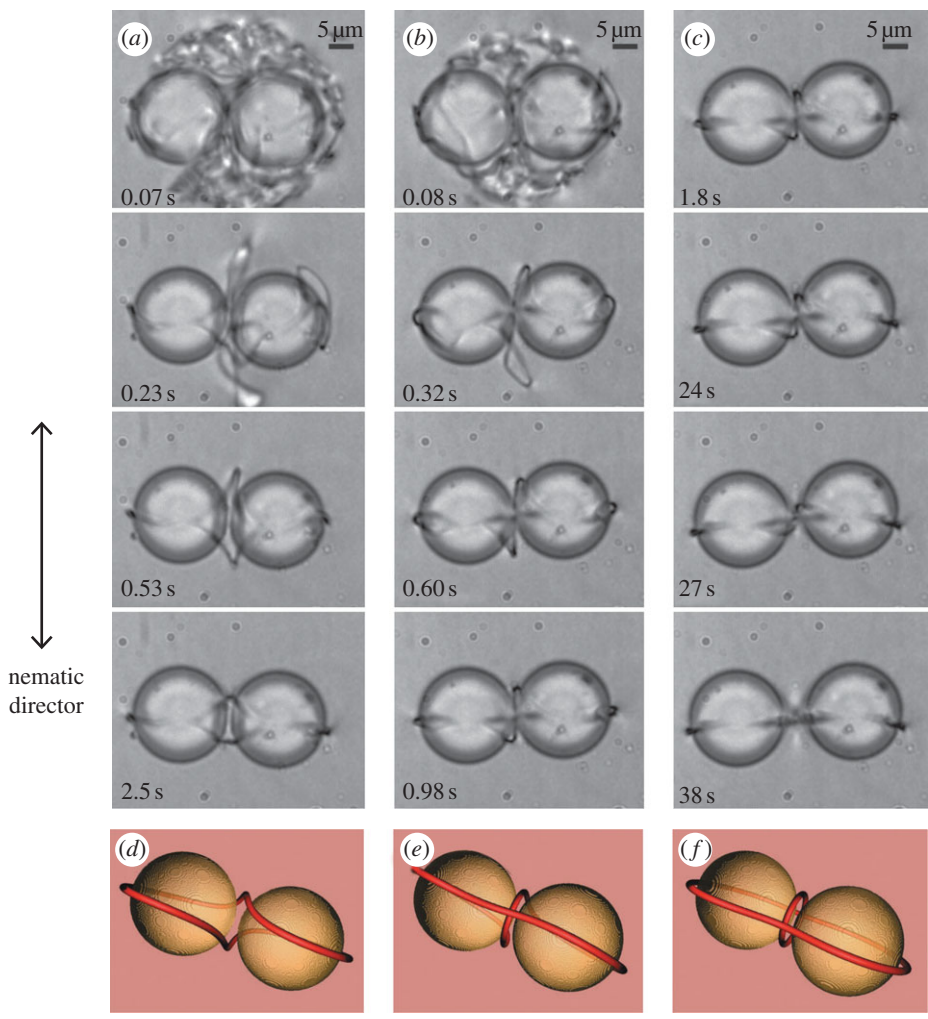


**Figure 4.** Entangled colloidal dimers in a nematic LC. (a) Figure-of-eight entanglement; (b) figure-of-omega entanglement; (c) entangled point defect, also called theta entanglement. (Online version in colour.)

#### 4. Entangled and knotted colloidal soft matter

It was recognized in 2006 that a couple of colloidal particles with normal surface anchoring of the nematic LC can be bound by a single-defect loop, entangling both particles as an elastic immaterial rope that encircles both particles [28–30]. This entanglement was first observed in laser-quenching experiments [31], where a pair of particles was positioned close to each other, and by using the strong light of the laser tweezers, the nematic LC around the particles was melted. However, when the light was switched off, a rapid thermal quenching of the nematic LC proceeded, producing lots of topological defect loops. In the course of time, all the defect loops but one, or in some cases two, were annihilated. In most cases, there was a single loop remaining, which encircled a colloidal pair in the form of a figure of eight, as presented in figure 4. The entanglement of a pair of colloidal particles is manifested in three different structures, illustrated in figure 4: (a) a figure of eight, (b) a figure of omega and (c) a figure of theta. While the figure of eight and the figure of omega are single loops of the winding number  $-1/2$  [26], the figure of theta is composed of two, separated, defect loops, each of the winding number  $-1/2$ . The difference here is that the single loop in the figure of eight or omega is twisted. Namely, the cross section of the  $-1/2$  disclination line has a threefold symmetry axis and the line is

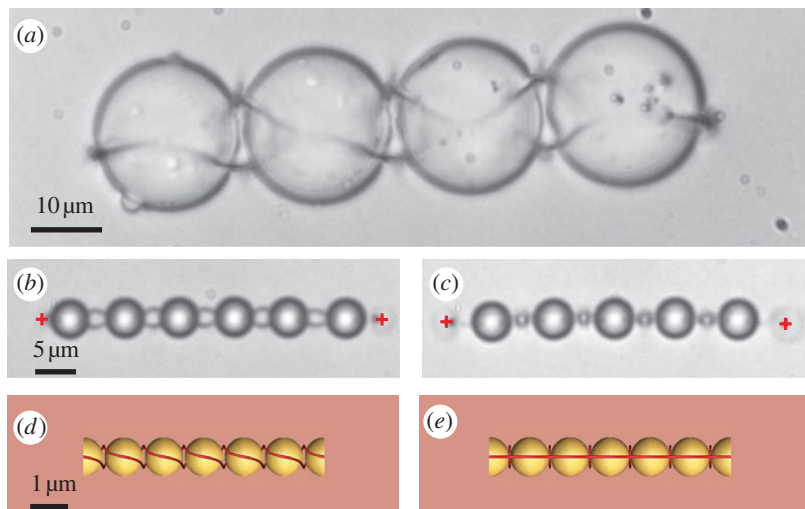


**Figure 5.** (a) Entangled colloidal chain in a planar nematic LC cell. Each particle is entangled with its neighbours by the figure-of-eight defect loop. (b, c) Entangled colloidal wires can be stretched with two traps of the laser tweezers. (d, e) Landau–de Gennes simulation of entangled colloidal wires. Courtesy of M. Skarabot and M. Ravnik. (Online version in colour.)

therefore not a structureless rope, but rather a belt with three sides. More precisely, it is a twisted, three-sided rope, similar to the Moebius two-sided belt. If one imagines travelling along the loop on one of the three sides of the defect line, then after one circulation one finds oneself on the other edge of the three-sided belt and so on. The number of loops and the spontaneous twisting of the defect loops raise a question about the topological charge that is supposedly carried by these structures. Interesting studies in this direction were performed recently, introducing the self-linking number for a description of the twisting of the disclination loops [32].

The binding colloidal-pair potential and the forces mediated by the entanglement are extremely strong, exceeding  $10.000 k_B T$  of energy for a colloidal particle of micrometre dimensions [31]. The force is string-like and shows little dependence when the two particles are stretched apart by the external force of the laser tweezers. This can easily be understood, because increasing the separation between the particles means that the total length of the loop is increased and also the energy stored in the loop is increased. The energy increase does not depend on the length of the loop, which means that the force needed to elongate the loop is constant. The experiments with an entangled colloidal pair stretched by the laser tweezers demonstrate, at least qualitatively, the string-like nature of the entanglement force. Entangled colloidal dimers are not the only stable one-dimensional structures. It is straightforward to demonstrate that an arbitrary number of colloidal particles can be added by simply inducing a fusion of the defect lines with the laser tweezers. In this case, the laser tweezers serve not only as a tool for grabbing and moving the particles, but also as a local, ‘microsurgical’ instrument. Namely, if the power of the laser tweezers is increased, the light is increasingly absorbed; this gives rise to a local temperature increase, thus locally softening and finally melting the LC. The molten region can be quite small and, if this melting is performed on the defect lines close to the colloidal particles, the lines can be ‘re-wired’ in a well-controlled way. Using this defect-rewiring technique, it is possible to assemble arbitrarily long and entangled colloidal wires using the particle-by-particle method, as shown in figure 5.

Colloidal entanglement is a phenomenon that is unique to LCs and cannot be realized in any other isotropic colloidal solvent. While one-dimensional entangled colloidal structures in planar nematic cells are easily realized, the search for two-dimensional entangled colloidal structures in planar nematic cells was not successful, in spite of theoretical predictions that such structures should be stable as well. A significant advancement was, however, demonstrated in nematic

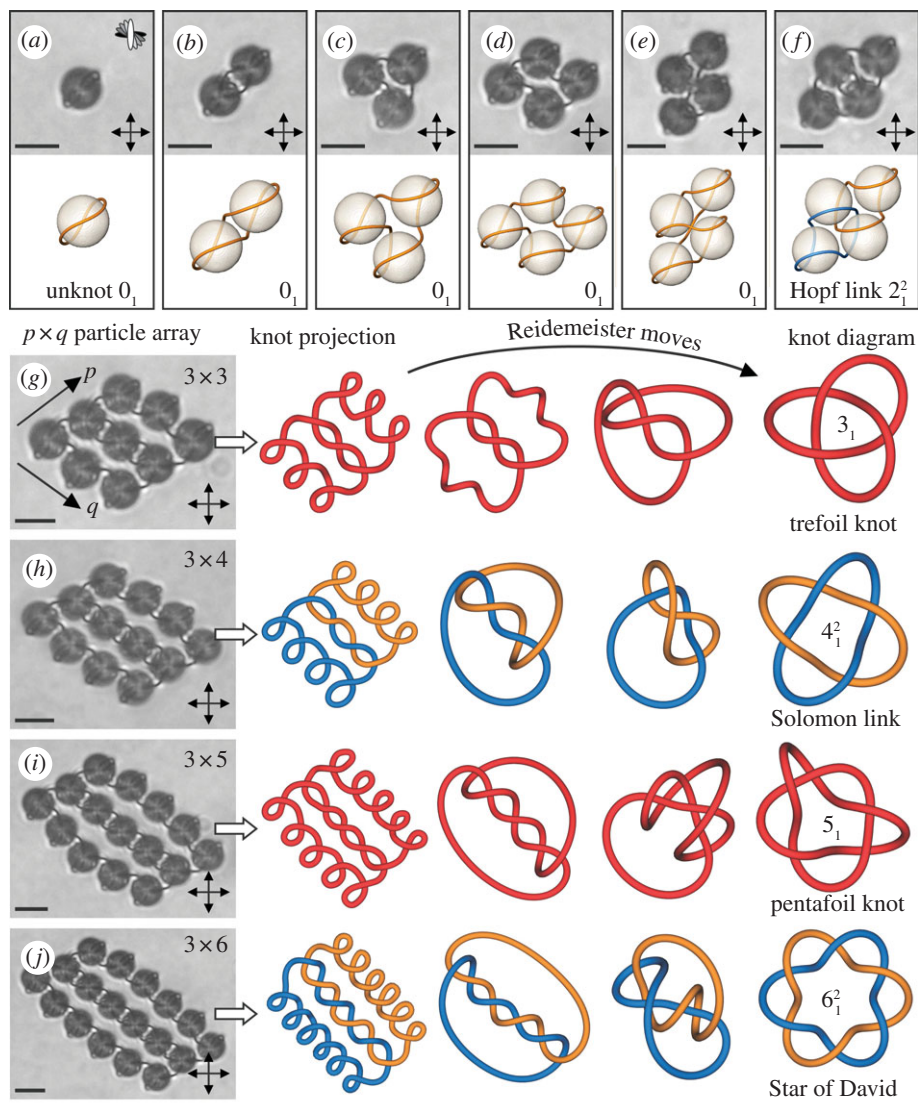


**Figure 6.** Knots and links in chiral nematic colloids. Topological defects appear in the form of closed loops that are linked and knotted around colloidal particles. Courtesy of U. Tkalec. (Online version in colour.)

colloids by taking a chiral nematic LC instead of a homogeneous, non-chiral nematic LC. Tkalec *et al.* [33] observed knots and links, formed by topological defect loops around colloidal particles in a chiral nematic LC. When colloidal particles with perpendicular surface alignment of LC molecules are inserted into a  $\pi/2$  twisted nematic cell with a thickness only slightly greater than the colloidal diameter, each colloidal particle is encircled by a  $-1/2$  disclination loop, as predicted theoretically by Terentjev [34] and analysed by Kuksenok *et al.* [35]. The disclination loop is also called a Saturn ring [36] and was observed in water–nematic dispersions [37] and nematic dispersions of glass microspheres [38]. When two such particles are positioned close to each other, their Saturn rings can be rewired using the laser tweezers to form a single-defect loop, encircling both particles in the form of a figure of eight [29]. And when the third colloidal particle is added, the loops can be rewired so that a single-defect loop entangles all three particles. The equilibrium positions of the centres of gravity of the particles are now not collinear, but are instead positioned in the corners of the triangle, as demonstrated in figure 6.

The entanglement changes dramatically as soon as we add the fourth particle, as shown in figure 6. Instead of a single-defect loop, two defect loops may appear, which are not separated, but interpenetrate each other, as demonstrated in figure 6f. The topological form of two ‘enchained’ or ‘linked’ loops is well known in the topology as the Hopf link. In Nature, the links are quite common topological forms, known for example in organic chemistry, where the interlinked molecular rings are called the ‘catenanes’ and interlocked molecules are known as the ‘rotaxanes’. More complex topological forms were obtained on regular arrays of ‘ $p \times q$ ’ colloidal particles, such as the trefoil knot on a  $3 \times 3$  particle array, the Solomon link on a  $3 \times 4$  array, etc., as presented in figure 6. In physics, links and knots are rare and have been observed directly in only a few experiments, such as the interference pattern of light, where the zero-intensity contour lines form knots and links of the electromagnetic field [39]. The knotting and linking of the defect loops in LCs seem to be particularly rich in chiral nematic colloids, as demonstrated in experiments with controlled chirality of the chiral nematic ‘solvent’ [40]. Chiral symmetry and the structure of the nematic LC, therefore, strongly promote the three-dimensional winding and propagation of disclination loops and lines inside the nematic LC, and it is expected that three-dimensional nematic colloidal superstructures, knotted and linked by the nematic defect loops, should be stable.

In summary, recent work on nematic and chiral nematic colloids has revealed a fascinating variety of forces between colloidal particles immersed into a nematic LC. These forces provide not only a very interesting platform for exploring the fundamental topology of the ordering field in nematics, but also indicate a possible application of nematic structural forces to design and assemble relatively complex colloidal structures and superstructures.

## 5. Optical microresonators and microlasers based on liquid-crystal dispersions and emulsions

At present, the microphotonic devices for directing and processing optical signals on a chip are produced from silicon using complex semiconductor technologies. In order to create and process the optical pulses, one has to be able not only to produce the optical pulses using controlled microlasers but also to launch them into the fibre networks, and then re-direct and detect them at a clock rate exceeding tens of gigahertz and beyond. The question is, whether we could do something similar using complex soft matter, in particular LC dispersions and emulsions. In order to do that we would have to prove that it is possible to create or self-assemble soft-matter microlasers, optical microcavities, fibres and detectors, etc. In addition, we would have to assemble these microphotonic elements into firmly bound photonic structures with complex architectures and well-defined photonic parameters.

There are at least two basic elements that are required to make an active photonic device: an optical microresonator and a microlaser. An optical microresonator is a microcavity that confines the electromagnetic field in the form of eigenwaves. There are two possible ways to confine the light in a small cavity: (i) by using the total internal reflection (TIR) of light at the surface of the cavity or (ii) by using a Bragg periodic dielectric structure. In the case of TIR, the microcavities are usually made in the form of a microsphere, microtoroid or a microdisc, produced from a high-index solid-state material [41]. In the conventional picture, the light is circulating inside the microresonator and bouncing off the walls owing to the TIR. If the light returns to the point of origin with the same phase, the conditions for resonance are met. These resonant optical waves are also called the whispering-gallery modes (WGMs), referring to the remarkable acoustic effect observed in domes [34]. The optical microresonators are the key elements for constructing optical devices, such as add-drop optical filters, routers, attenuators, etc. [42]. The light is coupled to the WGM resonators using tapered optical fibres that are positioned close to the microresonator. The overlapping of the evanescent fields of the microresonator and the fibre is required as well as the fine-tuning of the WGM eigenwaves to the frequency of the eigenwaves in the optical fibre for the resonant transport of light from the fibre to the resonator and back.

The second important microelement vital to the function of any optically active microdevice is the laser. There are two key elements of a microlaser: the optical microcavity providing the confinement of the light and the active medium producing the light via stimulated emission. The role of the optical microcavity is to re-direct the light that is emitted by light emitters back into the active matter, thus stimulating the emission of additional photons. Once the optical gain and the production of photons inside the cavity are exceeding the losses, the laser emission takes place. In soft matter, lasers were realized a long time ago in cholesteric LCs [43], ferroelectric smectic phases [44] and in blue phases [45]. In cholesteric lasers, thin layers of a cholesteric LC with large lateral dimensions are used and the lasing is stimulated by an external pumping pulsed laser of shorter wavelength. A cholesteric laser is therefore a dye laser in which the lasing wavelength is determined by the helical period of the cholesteric structure. The emission wavelength is positioned at the edge of the reflection band of the cholesteric.

It has recently been demonstrated that WGM tuneable optical microresonators and microlasers could be realized in LC emulsions, where a nematic or cholesteric LC is dispersed into an insoluble isotropic medium, such as water, polydimethyl-siloxane (PDMS), polymer, etc. Tuneable nematic microresonators have been reported by Humar *et al.* [46,47] in emulsions of microdroplets of the nematic LC E12 in PDMS. Because the surface anchoring of E12 at the PDMS interface is homeotropic, each nematic droplet adopts a radial configuration with a topological hedgehog defect in the centre (figure 7*a–c*). The extraordinary refractive index of E12 is  $n_e = 1.74$ , which is much higher than the refractive index of PDMS,  $n_s = 1.43$ . This means that the E12 radial microdroplet is a WGM microresonator for EM eigenwaves with the electric field pointing towards the centre of the droplet, i.e. along the long molecular axis of the nematic. The WGM spectrum of the radial nematic microdroplet is readily observed by dissolving a small amount of a fluorescent dye inside the LC. After the excitation of the fluorescent dye with a pulsed short-wavelength external laser, WGMs are created inside the nematic microdroplet from the emitted fluorescent light. The WGMs are clearly visible under an optical microscope (as illustrated in figure 7*d*) in the form of a fluorescent ring with two bright spots at opposite positions. The spectrum of light, leaking from the microdroplet in the form of a ring, demonstrates a set of optical resonances, corresponding to individual WGMs [46]. The resonances are very sharp, with a bandwidth of less than 0.1 nm, corresponding to 15 GHz. The position and splitting of the WGM resonances depend on the birefringence of the LC, and that makes it possible to shift the resonances using an external electric field. When the field is applied to the radial nematic microdroplet, it couples to the dielectric anisotropy of the nematic molecules and induces significant elastic distortion inside the microdroplet. This reorientation causes changes in the optical path of the circulating WGMs, therefore changing the conditions for the resonances to occur. As a result, the positions of the WGMs change continuously under an applied electric field, which makes it possible to tune the WGMs electrically. The electric tuning of the WGM resonances in a radial nematic droplet is presented in figure 7*e*. The tuning capability is very large, and the resonances can be shifted by  $\approx 20$  nm at a driving electric field of only  $2 \text{ V } \mu\text{m}^{-1}$ . The radial nematic WGM microresonators with the fluorescent dye are not only tuneable optical resonators, but they also emit laser light when there is enough optical energy supplied by the pumping pulsed light. If the pumping energy is increased, the WGM resonances start to grow strongly above some threshold energy [47].

While the non-chiral nematic LC provides the self-assembly of tuneable WGM microresonators and microlasers, the chiral nematic LC provides the self-assembly of another interesting LC microdevice, i.e. the three-dimensional microlaser, first demonstrated by Humar & Mušević [48]. The microlaser is produced by dispersing a chiral nematic LC with a small amount of fluorescent dye in an isotropic insoluble medium, such as water or glycerine. Surfactants may be added to ensure planar anchoring of the LC molecules at the interface. Owing to immiscibility, chiral nematic microdroplets of a perfect spherical shape are spontaneously formed in the carrier isotropic liquid (figure 8*a–c*). Because of the planar surface anchoring, the internal structure is such that the helical modulation of the chiral nematic LC extends from the centre of the droplet to the surface, illustrated in figure 8*b*. Optically, such a droplet is a birefringent onion Bragg

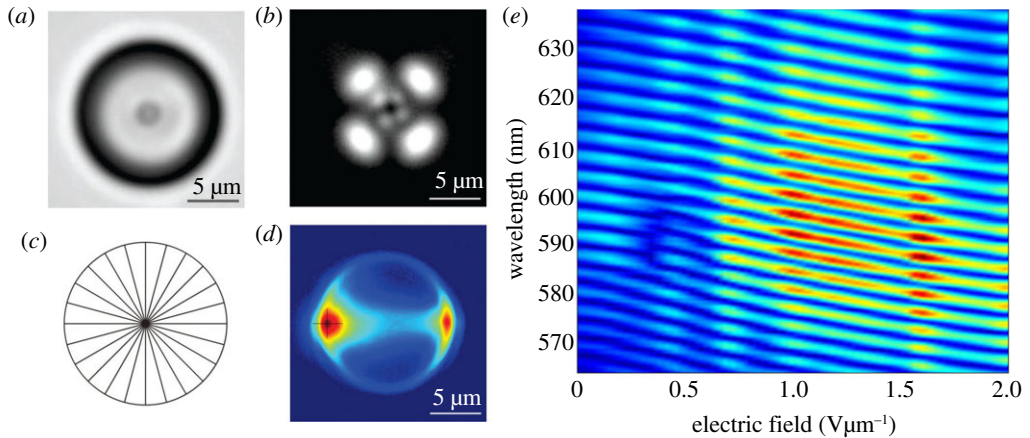


**Figure 7.** (a–d) A microdroplet of the nematic LC in PDMS. (a) Droplet of 5CB in PDMS, as observed without polarizers. (b) The same droplet as in (a), observed under crossed polarizers. A topological defect (radial hedgehog) is visible in the centre of the droplet, encircled by a thin interference ring. (c) The nematic LC forms the radial structure with a hedgehog defect in the centre. (d) A fluorescent ring due to WGMs circulating inside the droplet is observed, when the fluorescence is excited by shining pumping light onto the droplet (black cross). (e) Electric field tuning of the WGM resonances in a 5CB microdroplet. (Online version in colour.)

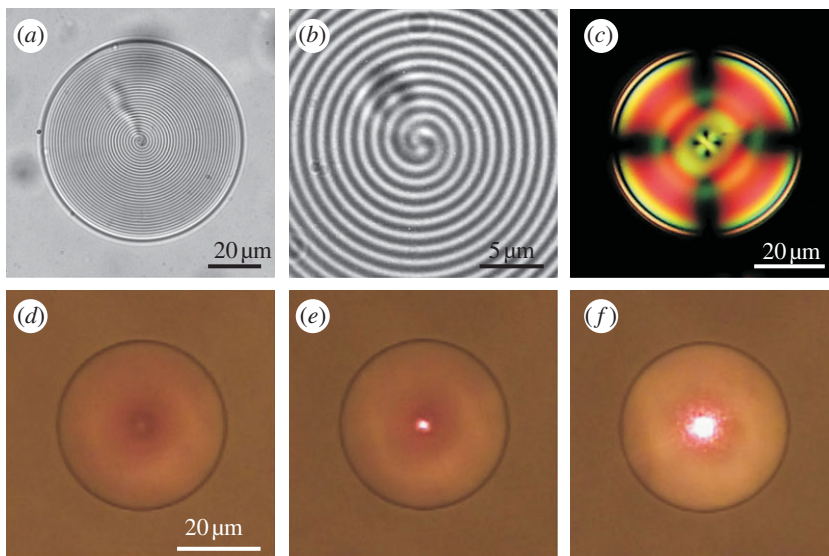


**Figure 8.** Three-dimensional microlaser, self-assembled from a chiral nematic droplet in an insoluble carrier fluid. (a) Micrograph of a droplet under an optical microscope. Defect line extending from the centre to the surface is visible. (b) When the helical period of the cholesteric is large, an onion-like structure of the birefringent cholesteric is clearly visible. (c) When the helical period is in the range of visible light, the cholesteric droplet exhibits vivid birefringent colours between the crossed polarizers. (d–f) Micrographs showing lasing of the droplet. (d) Below the threshold, there is little light emitted from the droplet. When the intensity of the pumping light is increased, the droplet starts lasing above the threshold, which is just about (e). (Online version in colour.)

microresonator. This kind of resonator can be considered as a concentric stack of dielectric shells with an alternating high and low refractive index. As it is filled with an active medium, the lasing is observed above some energy threshold when the pumping energy is increased (figure 8d–f). It has been demonstrated that a three-dimensional microlaser based on chiral nematic colloids indeed emits light in all directions, thus providing a coherent point source of monochromatic

light. The laser itself is a band-edge type, as the emitted wavelength is positioned at the edge of the one-dimensional photonic gap of the chiral nematic material used [43]. The emitted wavelength can therefore be tuned by temperature and possibly external electric and magnetic fields. Recently, polymerized three-dimensional microlasers have been demonstrated [49], as well as lasing in paintable dye-doped chiral nematic emulsions [50].

## 6. Topology and photonics of knotted soft matter

In conclusion, the developments in the field of nematic colloids and emulsions in recent years have demonstrated the unusually rich phenomena in these complex, soft-matter materials, ranging from purely fundamental topological phenomena, such as the knotting and linking of the ordering field in nematic colloids, to novel optical phenomena in nematic emulsions. This richness is a direct consequence of the complexity of the nematic ordering field  $\underline{S}(\vec{r})$  in comparison with the electromagnetic field, which mediates the interactions in conventional, water-based colloids. An important aspect here is the chirality of the ordering field, which promotes the appearance of non-trivial topological phenomena, such as knotting and the linking of topological defects. In addition, the richness of the nematic colloids is directly related to our ability to control the anchoring of the nematic ordering field at the surfaces of the colloidal particles. Without this interaction at the molecular level, there would be no topological defects and colloidal interactions.

The field of nematic colloids has evolved as an unusual mixture of pure and applied phenomena, which must be our guide for future studies. We anticipate that, from the perspective of fundamental science, studies of topological defects that surround objects with different geometrical shapes is a very promising direction. This includes fibres, which are topologically equivalent to spheres, but might promote the stability of unusual topological states because of their one-dimensional character. Another example is defects on topologically more complex objects, such as the toroids in chiral nematics, etc. Here, the challenge is to advance the methods of microfabrication for topologically non-trivial micro-objects, using e-beam lithography or a two-photon polymerization technique in three dimensions. Finally, the microfabrication of three-dimensional matrices with a controlled geometry [51] is a very promising route to the creation of new materials, where the topology might play an important role. This can lead to novel, soft-matter materials, where the functions of the materials will be determined by their topology. On the other hand, there is an obvious interplay between topology as a fundamental phenomenon and the photonic properties of nematic colloids and emulsions. The combination of the two might lead to novel microphotonic devices and even systems based on complex soft matter, where the nematic carrier would provide the structural forces that bind the various microphotonic elements into a functional unity. This combination may be realized by using new experimental techniques that have been developed for the manipulation of colloidal particles during the past 10 years, such as optical and magnetic tweezers, optoelectronic tweezers and microfluidic systems. New colloidal structures and superstructures are expected to emerge based on three-dimensional polymer scaffolds, produced by a two-photon polymerization technique. These structures need not be made of hard-matter colloidal inclusions, but could be based on emulsions where two or more immiscible (simple and complex) fluids are used to create the three-dimensional structures. Regarding the photonic properties of confined LCs, a number of future challenges are foreseen, such as the optically driven fast and ultrafast dynamics of the nematic ordering field, plasmonics and the control of the optical properties by light. Here, the concepts will most likely be based on a fluorescence mechanism, which provides fast response and optical control.

I would like to thank Miha Škarabot, Miha Ravnik, Slobodan Žumer, Uroš Tkalec, Matjaž Humar, Ulyana Ognysta and Andriy Nych for their valuable contribution to this work. The work was supported by the Slovenian Research Agency (ARRS) under the project J1-3612.

1. Yablonovitch E, Gmitter TJ. 1989 Photonic band structure: the face-centered-cubic case. *Phys. Rev. Lett.* **63**, 1950–1953. (doi:10.1103/PhysRevLett.63.1950)
2. van Blaaderen A, Ruel R, Wiltzius P. 1997 Template-directed colloidal crystallization. *Nature* **385**, 321–324. (doi:10.1038/385321a0)
3. Aoki K, Miyazaki HT, Hirayama H, Inoshita K, Baba T, Sakoda K, Shinya N, Aoyagi Y. 2003 Microassembly of semiconductor three-dimensional photonic crystals. *Nat. Mater.* **2**, 117–121. (doi:10.1038/nmat802)
4. Chiou PY, Ohta AT, Wu MC. 2005 Massively parallel manipulation of single cells and microparticles using optical images. *Nature* **436**, 370–372. (doi:10.1038/nature03831)
5. Mirkin CA, Letsinger RL, Mucic RC, Storhoff JJ. 1996 A DNA-based method for rationally assembling nanoparticles into macroscopic materials. *Nature* **382**, 607–609. (doi:10.1038/382607a0)
6. Liang D, Bowers JE. 2010 Recent progress in lasers on silicon. *Nat. Photonics* **4**, 511–517. (doi:10.1038/nphoton.2010.167)
7. Poulin P, Stark H, Lubensky TC, Weitz DA. 1997 Novel colloidal interactions in anisotropic fluids. *Science* **275**, 1770–1774. (doi:10.1126/science.275.5307.1770)
8. Poulin P, Cabuil V, Weitz DA. 1997 Direct measurement of colloidal forces in an anisotropic solvent. *Phys. Rev. Lett.* **79**, 4862–4865. (doi:10.1103/PhysRevLett.79.4862)
9. Takahashi K, Ichikawa M, Kimura Y. 2008 Force between colloidal particles in nematic liquid crystals studied by optical tweezers. *Phys. Rev. E* **77**, 020703. (doi:10.1103/PhysRevE.77.020703)
10. Yada M, Yamamoto J, Yokoyama H. 2004 Direct observation of anisotropic interparticle forces in nematic colloids with optical tweezers. *Phys. Rev. Lett.* **92**, 185501. (doi:10.1103/PhysRevLett.92.185501)
11. Muševič I, Škarabot M, Tkalec U, Ravnik M, Žumer S. 2006 Two dimensional nematic colloidal crystals self-assembled by topological defects. *Science* **313**, 954–958. (doi:10.1126/science.1129660)
12. Takahashi K, Ichikawa M, Kimura Y. 2008 Direct measurement of force between colloidal particles in a nematic liquid crystal. *J. Phys.: Condens. Matter* **20**, 075106. (doi:10.1088/0953-8984/20/7/075106)
13. Noel CM, Bossis G, Chaze A-M, Giulieri F, Laci S. 2006 Measurement of elastic forces between two colloidal particles in a nematic liquid crystal. *Phys. Rev. Lett.* **96**, 217801. (doi:10.1103/PhysRevLett.96.217801)
14. Smalyukh II, Lavrentovich OD, Kuzmin AN, Kachynski AV, Prasad PN. 2005 Elasticity-mediated self-organization and colloidal interactions of solid spheres with tangential anchoring in a nematic liquid crystal. *Phys. Rev. Lett.* **95**, 157801. (doi:10.1103/PhysRevLett.95.157801)
15. Vilfan M, Osterman N, Čopič M, Ravnik M, Žumer S, Kotar J, Babič D, Poberaj I. 2008 Confinement effect on interparticle potential in nematic colloids. *Phys. Rev. Lett.* **101**, 237801. (doi:10.1103/PhysRevLett.101.237801)
16. Škarabot M, Ravnik M, Žumer S, Tkalec U, Poberaj I, Babič D, Osterman N, Muševič I. 2007 Interactions of quadrupolar nematic colloids. *Phys. Rev. E* **76**, 051406. (doi:10.1103/PhysRevE.76.051406)
17. Ognysta U, Nych A, Nazarenko V, Muševič I, Škarabot M, Ravnik M, Žumer S, Poberaj I, Babič D. 2008 2D interactions and binary crystals of dipolar and quadrupolar nematic colloids. *Phys. Rev. Lett.* **100**, 217803. (doi:10.1103/PhysRevLett.100.217803)
18. Škarabot M, Ravnik M, Žumer S, Tkalec U, Poberaj I, Babič D, Osterman N, Muševič I. 2008 Two-dimensional dipolar nematic colloidal crystals. *Phys. Rev. E* **77**, 031705. (doi:10.1103/PhysRevE.77.031705)
19. Škarabot M, Ravnik M, Žumer S, Tkalec U, Poberaj I, Babič D, Osterman N, Muševič I. 2008 Hierarchical self-assembly of nematic colloidal superstructures. *Phys. Rev. E* **77**, 061706. (doi:10.1103/PhysRevE.77.061706)
20. Tkalec U, Ravnik M, Žumer S, Muševič I. 2009 Vortexlike topological defects in nematic colloids: chiral colloidal dimers and 2D crystals. *Phys. Rev. Lett.* **103**, 127801. (doi:10.1103/PhysRevLett.103.127801)

21. Fukuda J-i, Yokoyama H. 2005 Separation-independent attractive force between like particles mediated by nematic-liquid-crystal distortions. *Phys. Rev. Lett.* **94**, 148301. (doi:10.1103/PhysRevLett.94.148301)
22. Lubensky TC, Pettey D, Currier N, Stark H. 1998 Topological defects and interactions in nematic emulsions. *Phys. Rev. E* **57**, 610–625. (doi:10.1103/PhysRevE.57.610)
23. Mermin ND. 1979 The topological theory of defects in ordered media. *Rev. Mod. Phys.* **51**, 591–648. (doi:10.1103/RevModPhys.51.591)
24. Trebin HR. 1982 The topology of non-uniform media in condensed matter physics. *Adv. Phys.* **31**, 195–254. (doi:10.1080/00018738200101458)
25. Kurik MV, Lavrentovich OD. 1988 Defects in liquid crystals: homotopy theory and experimental studies. *Sov. Phys. Usp.* **31**, 196–224. (doi:10.1070/PU1988v031n03ABEH005710)
26. Stark H. 2001 Physics of colloidal dispersions in nematic liquid crystals. *Phys. Rep.* **351**, 387–474. (doi:10.1016/S0370-1573(00)00144-7)
27. Čopar S, Žumer S. 2012 Topological and geometric decomposition of nematic textures. *Phys. Rev. E* **85**, 031701. (doi:10.1103/PhysRevE.85.031701)
28. Guzmán O, Kim EB, Grollau S, Abbott NL, de Pablo JJ. 2003 Defect structure around two colloids in a liquid crystal. *Phys. Rev. Lett.* **91**, 235507. (doi:10.1103/PhysRevLett.91.235507)
29. Žumer S. 2006 Book of abstracts. In *21st Int. Liquid Crystal Conf., Keystone, CO, 2–7 July 2006*. Littleton, CO: Kinsley & Associates, LLC.
30. Araki T, Tanaka H. 2006 Colloidal aggregation in a nematic liquid crystal: topological arrest of particles by a single-stroke disclination line. *Phys. Rev. Lett.* **97**, 127801. (doi:10.1103/PhysRevLett.97.127801)
31. Ravnik M, Škarabot M, Žumer S, Tkalec U, Poberaj I, Babič D, Osterman N, Muševič I. 2007 Entangled nematic colloidal dimers and wires. *Phys. Rev. Lett.* **99**, 247801. (doi:10.1103/PhysRevLett.99.247801)
32. Čopar S, Žumer S. 2011 Nematic braids: topological invariants and rewiring of disclinations. *Phys. Rev. Lett.* **106**, 177801. (doi:10.1103/PhysRevLett.106.177801)
33. Tkalec U, Ravnik M, Čopar S, Žumer S, Muševič I. 2011 Reconfigurable knots and links in chiral nematic colloids. *Science* **333**, 62–65. (doi:10.1126/science.1205705)
34. Terentjev EM. 1995 Disclination loops, standing alone and around solid particles in nematic liquid crystals. *Phys. Rev. E* **51**, 1330–1337. (doi:10.1103/PhysRevE.51.1330)
35. Kuksenok OV, Ruhwandl RW, Shiyonovskii SV, Terentjev EM. 1996 Director structure around a colloid particle suspended in a nematic liquid crystal. *Phys. Rev. E* **54**, 5198–5203. (doi:10.1103/PhysRevE.54.5198)
36. Ruhwandl RW, Terentjev EM. 1997 Monte Carlo simulation of topological defects in the nematic liquid crystal matrix around a spherical colloid particle. *Phys. Rev. E* **56**, 5561–5565. (doi:10.1103/PhysRevE.56.5561)
37. Mondain-Monval O, Dedieu JC, Gulik-Krzywicki T, Poulin P. 1999 Weak surface energy in nematic dispersions: Saturn ring defects and quadrupolar interactions. *Eur. Phys. J. B* **12**, 167–170. (doi:10.1007/s100510050992)
38. Gu Y, Abbott NL. 2000 Observation of Saturn-ring defects around solid microspheres in nematic liquid crystals. *Phys. Rev. Lett.* **85**, 4719–4722. (doi:10.1103/PhysRevLett.85.4719)
39. Dennis MR, King RP, Jack B, O'Holleran K, Padgett MJ. 2010 Isolated optical vortex knots. *Nat. Phys.* **6**, 118–121. (doi:10.1038/nphys1504)
40. Jampani VSR, Škarabot M, Ravnik M, Čopar S, Žumer S, Muševič I. 2011 Colloidal entanglement in highly twisted chiral nematic colloids: twisted loops, Hopf links, and trefoil knots. *Phys. Rev. E* **84**, 031703. (doi:10.1103/PhysRevE.84.031703)
41. Armani DK, Kippenberg TJ, Spillane SM, Vahala KJ. 2003 Ultra-high-Q toroid microcavity on a chip. *Nature* **421**, 925–928. (doi:10.1038/nature01371)
42. Kress BC, Meyrueis P. 2009 *Applied digital optics*. Chichester, UK: John Wiley and Sons Ltd.
43. Coles H, Morris S. 2010 Liquid-crystal lasers. *Nat. Photonics* **4**, 676–685. (doi:10.1038/nphoton.2010.184)
44. Ozaki M, Kasano M, Ganzke D, Haase W, Yoshino K. 2002 Mirrorless lasing in a dye-doped ferroelectric liquid crystal. *Adv. Mater.* **14**, 306–309. (doi:10.1002/1521-4095(20020219)14:4<306::AID-ADMA306>3.0.CO;2-1)
45. Cao W, Muñoz A, Palffy-Muhoray P, Taheri B. 2002 Lasing in a three-dimensional photonic crystal of the liquid crystal blue phase II. *Nat. Mater.* **1**, 111–113. (doi:10.1038/nmat727)
46. Humar M, Ravnik M, Pajk S, Muševič I. 2009 Electrically tunable liquid crystal optical microresonators. *Nat. Photonics* **3**, 595–600. (doi:10.1038/nphoton.2009.170)

47. Humar M, Mušević I. 2011 Surfactant sensing based on whispering-gallery-mode lasing in liquid-crystal microdroplets. *Opt. Express* **19**, 19 836–19 844. (doi:10.1364/OE.19.019836)
48. Humar M, Mušević I. 2010 3D microlasers from self-assembled cholesteric liquid-crystal microdroplets. *Opt. Express* **18**, 26 995–27 003. (doi:10.1364/OE.18.026995)
49. Cipparrone G, Mazzulla A, Pane A, Hernandez RJ, Bartolino R. 2011 Chiral self-assembled solid microspheres: a novel multifunctional microphotonic device. *Adv. Mat.* **23**, 5773–5778. (doi:10.1002/adma.201102828)
50. Gardiner DJ, Morris SM, Hands PJW, Mowatt C, Rutledge R, Wilkinson TD, Coles HJ. 2011 Paintable band-edge liquid crystal lasers. *Opt. Express* **19**, 2432–2439. (doi:10.1364/OE.19.002432)
51. Serra F, Vishnubhatla KC, Buscaglia M, Cerbino R, Osellame R, Cerullo G, Bellini T. 2011 Topological defects of nematic liquid crystals confined in porous networks. *Soft Matter* **7**, 10 945–10 950. (doi:10.1039/c1sm05813d)









